ISSN 1061-3862, International Journal of Self-Propagating High-Temperature Synthesis, 2016, Vol. 25, No. 1, pp. 23–29. © Allerton Press, Inc., 2015.

Low-Temperature Solution-Combustion Synthesis and Magneto-Structural Characterization of Polycrystalline $La_{1-x}Ag_yMnO_3$ ($y \le x$) Manganites[1]

C. O. Ehi-Eromosele[a], B. I. Ita[a,b], A. Edobor-Osoh[a], and F. E. Ehi-Eromosele[c]

[a] *Department of Chemistry, Covenant University, PMB 1023, Ota, Nigeria*

[b] *Department of Pure and Applied Chemistry, University of Calabar, Calabar, Nigeria*

[c] *Department of Mechanical Engineering, University of Benin, Benin City, Nigeria*

e-mail: cyril.ehi-eromosele@covenantuniversity.edu.ng

Received September 16, 2015

Abstract—Silver is known to be a highly mobile (low-soluble) component in Ag-doped perovskite manganites and hence several non-perovskite phases can exist in silver doped manganite perovskites with most synthetic routes making its synthesis to be problematic. In search of soft synthesis route, the low temperature combustion synthesis and magneto-structural studies of polycrystalline $La_{1-x}Ag_yMnO_3$ ($y \le x$) ceramic manganites using glycine as a fuel is reported. The sintered powders were characterized by X-Ray Diffraction (XRD), Scanning Electron Microscopy (SEM), Energy Dispersive X-ray (EDAX) analysis, Thermo Gravimetric Analysis (TGA) and Vibrating Scanning Magnetometer (VSM) measurements. XRD patterns showed formation of mainly single rhombohedral perovskite phase for the $La_{0.8}Ag_{0.15}MnO_3$ sample and an admixture of secondary phases with $La_{0.8}Ag_{0.1}MnO_3$ and $La_{0.8}Ag_{0.2}MnO_3$ samples. The distinct microstructure and higher magnetic properties observed for $La_{0.8}Ag_{0.15}MnO_3$ sample compared to the other samples were discussed based on the XRD results.

Keywords: solution-combustion synthesis, perovskite manganites, magnetic properties

DOI: 10.3103/S1061386216010040

INTRODUCTION

In the past two decades, perovskite manganites with the general formula $R_{1-x}A_xMnO_3$ (where R is a rare earth cation and A is doping cation) have been extensively investigated because of their interesting physical properties and potential applications [1–6]. Largely, the motivation for these studies stems from
1 the possible utility of colossal-magnetoresistance (CMR) and magnetocaloric (MC) properties in the perovskite manganites at low field and room temperature [7]. The substitution of the rare earth cations with monovalent cations (Ag^+, Na^+, K^+) in manganites are of particular interest because it leads to the change not only of the valence of Mn ions, like the divalent elements doping, but also to the A-site cation radius and A-site size disorder and thus of the magnetic and electrical behavior [8]. Particularly, silver-doped manganites has been shown to manifest giant MC effect which is comparable to that observed in the best MC materials with a maximum at room temperature and possess a high sensitivity of the resistance to a magnetic field at the same temperature [9–11]. Recently, silver doped perovskite manganites have been exploited as new materials with tunable Curie temperature (T_c) to be used as heat sources for temperature-controlled magnetic hyperthermia [12–15]. It has been shown that varying the silver content allows one to tune the T_c of these materials to the therapeutic hyperthermia temperature range of about 42–48°C.

In manganites, there is the possibility of inducing ferromagnetism and metal type conduction by silver doping, substituting lanthanum vacancies in the perovskite parent compound $LaMnO_3$ which is antiferromagnetic to form stoichiometric manganite with a general formula $La_{1-x}Ag_xMnO_3$. Also, ferromagnetism and metal type conduction can be induced by creating lanthanum vacancies along with silver doping to form non-stoichiometric manganite compositions with a general formula $La_{1-x}Ag_yMnO_3$ ($y < x$). Initially, although there were doubts of the insertion of silver ions in the perovskite lattice [16, 17], there is now experimental evidence for silver doping in the La-site sublattice of $La_{1-x}MnO_{3+\delta}$ [18]. However, the available information in literature on the amounts of silver doping allowable in the La-site sublattice of $La_{1-x}MnO_{3+\delta}$ for the crystallization of a pure perovskite phase with no secondary phase is rather conflicting. While some studies using different synthetic

[1] The article is published in the original.

routes [10, 18, 19] reveal a single phase rhombohedral perovskites for $x < 0.2$ and an admixture of secondary phases (mainly metallic silver) for $x > 0.2$; other studies using the solid state and sol-gel synthesis [17, 18–22] report that there are other peaks (mainly metallic silver peaks with very small intensities) in the XRD of silver doped lanthanum manganites irrespective of the amounts of silver present. Recently, another study using hydrothermal synthesis [23] reported the formation of Ag_2O_3 phase for $x > 0.04$ along with the perovskite phase. From the foregoing, it is very clear that several non-perovskite phases could exist in silver doped manganite perovskites with most synthetic routes making its synthesis to be problematic.

Silver is known to be a highly mobile (low-soluble) component in perovskite manganites [18] and hence soft synthesis conditions are required. Melnikov et al. [13] reported that the vacancies in the A-sublattice of the perovskite structure $La_{1-x}MnO_{3+d}$ can be filled by Ag^+ ions under soft conditions of synthesis. Also, a rapid solution combustion synthesis using oxalyl dihydrazide as a fuel and followed by calcinations at 800°C for 12 h has been used in the synthesis of pure perovskite phase $La_{1-x}Ag_xMnO_3$ ($x \le 0.15$) [24]. Solution combustion method is an alternative low temperature initiated route to prepare fine-grained oxide powders. It makes possible the rapid synthesis of several ceramic materials without the prolonged high temperature treatment of sintering [25]. In combustion synthesis, it is well known that nature of fuel plays an important role in determining the phase, morphology, and magnetic properties of the final product. In most combustion synthesis, glycine fuel is preferred to initiate the combustion reaction because of its high negative combustion heat hence; high sintering temperature is not required. There is paucity of reports in literature on silver-doped lanthanum manganites synthesized through the combustion route. In the present study, we report for the first time, to the best of our knowledge, on low-temperature combustion synthesis of nanocrystalline $La_{1-x}Ag_yMnO_3$ ($y \le x$) manganites by using glycine as a fuel.

2. EXPERIMENTAL

2.1. Combustion Synthesis

Polycrystalline samples of $La_{1-x}Ag_yMnO_3$ ($y \le x$) with nominal y values of 0.1, 0.15, and 0.2 have been prepared by the solution-combustion synthetic route using glycine as a fuel. In the synthesis of the different composition of $La_{1-x}Ag_yMnO_3$, fuel stoichiometric composition was used. Fuel stoichiometric composition was employed because optimum glycine is required to complex the metal cations, increasing their solubility and preventing selective precipitation as the water evaporates. For $y = 0.1$ sample ($La_{0.8}Ag_{0.1}MnO_3$), 3.46 g $La(NO_3)_3 \cdot 6H_2O$ (99.9% pure from Alfa Aesar, USA), 0.17 g $AgNO_3$ (99.9 + % purity from Aldrich), 2.51 g $Mn(NO_3)_2 \cdot 4H_2O$ (99.9 + % purity from Aldrich) and 1.88 g glycine (SD Fine Chem. Ltd, Mumbai) were dissolved in 20 mL of distilled water and the solutions were heated to 80°C to form a viscous gel of precursors under magnetic stirring. After that, the gel was transferred to a pre-heated coil (300°C). Finally, after a short moment, the solution precursors boiled, swelled, evolved a large amount of gases and ignited, followed by the yielding of puffy black products. The auto combusted powder was annealed at 800°C for 5 h in air and used for further characterization. Similarly, for $y = 0.15$ sample ($La_{0.8}Ag_{0.15}MnO_3$), same procedures were followed except that 0.26 g $AgNO_3$ and 1.90 g glycine were used as precursors while for $y = 0.2$ sample ($La_{0.8}Ag_{0.2}MnO_3$), 0.34 g $AgNO_3$ and 1.92 g glycine were used.

2.2. Characterization Methods

The precursor gel was characterized by TGA by means of a NETZSCH (Geratebau, Germany) simultaneous thermal analyzer at a temperature range of 30–1000°C in air with a heating rate of 10°C/min. The X-ray diffractograms of the annealed powders were recorded using an X-ray diffractometer (D8 Advance, Bruker, Germany), equipped with a CuK_α radiation source ($\lambda = 1.5406$ Å) and the crystallite size (D) is calculated from X-ray line broadening of the (110) diffraction peak using the well-known Scherrer relation:

$$D = \frac{0.9\lambda}{\beta \cos\theta}, \quad (1)$$

where β is the full width at half maximum of the strongest intensity diffraction peak (311), λ is the wavelength of the radiation, and θ is the angle of the strongest characteristic peak. The surface morphology and chemical composition were characterized by field-emission scanning electron microscopy (FEI NOVA NANO SEM 600 microscope). The magnetic characterizations were carried out with a Vibrating Scanning Magnetometer (VSM) (Lake Shore Cryotronics-7400) under the applied field of ±20 000 G at room temperature.

3. RESULTS AND DISCUSSION

3.1. Combustion Reaction

Assuming complete combustion, the general equation for the formation of $La_{1-x}Ag_yMnO_3$ ($y \le x$) nanoparticles can be written as follows:

$$\begin{aligned}(1-x)La(NO_3)_3(aq) + yAgNO_3(aq) \\ + Mn(NO_3)_2(aq) + NH_2CH_2COOH(aq) \\ + (9.99-10)O_2 \rightarrow La_{1-x}Ag_yMnO_3(aq) \\ + CO_2(g)\uparrow + H_2O(g)\uparrow + N_2(g)\uparrow.\end{aligned} \quad (2)$$

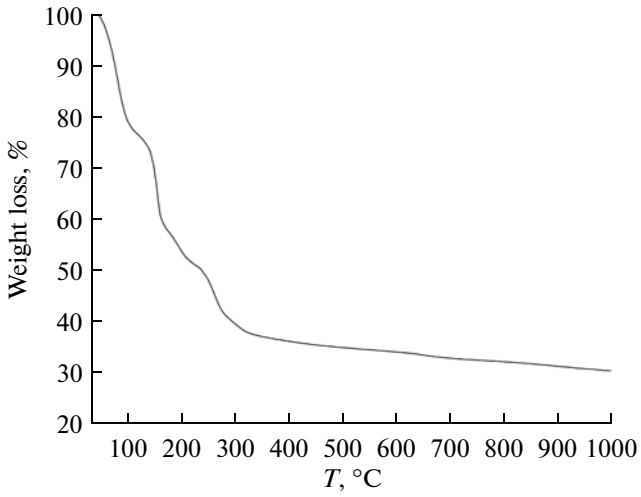

Fig. 1. TGA curve for the precursor gel of $La_{0.8}Ag_{0.15}MnO_3$ sample.

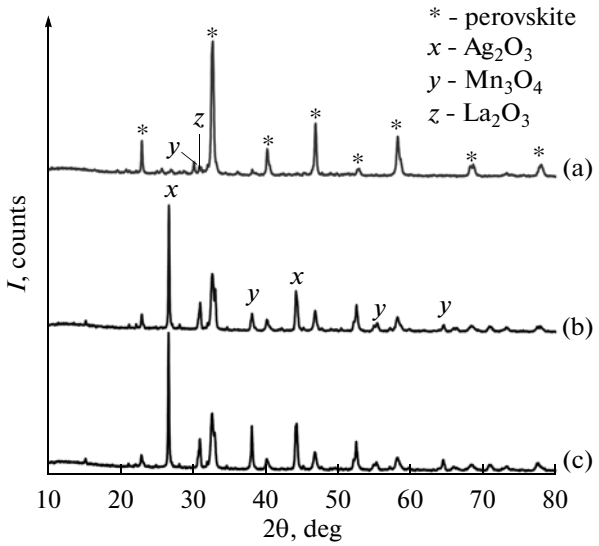

Fig. 2. XRD patterns of (a) $La_{0.8}Ag_{0.15}MnO_3$, (b) $La_{0.8}Ag_{0.1}MnO_3$, and (c) $La_{0.8}Ag_{0.2}MnO_3$ samples.

The mixing of the precursors in water resulted in a colorless solution which turned sooty black after combustion. In all samples, the combustion types were flamy combustion. After annealing at 800°C for 5 h, the powders became finer and were used for further characterizations.

3.2. Thermogravimetric Analysis

TGA was used to study the thermal evolution of the precursors to monitor the combustion process. The TGA curve for the stoichiometric precursor gel (for $La_{0.8}Ag_{0.15}MnO_3$ sample) was recorded in a temperature range of 35–1000°C and it is shown in Fig. 1. The TGA curve shows three weight loss processes at temperatures 35–110°C (22%), 110-220°C (26%) and 220–325°C (14%) with a total weight loss of 62%. The first weight loss is due to complete evaporation of water and organic contents in the precursor gel. The weight loss of 26% was attributed to the rapid chemical reaction between the metal nitrates and glycine. The third weight loss was attributed to the burning of the residual organic components. Thereafter, no significant weight loss was observed indicating the formation of a perovskite phase with a yield of about 34%. The thermogram shows stability above 700°C hence, ~700°C appears to be the phase formation temperature of the sample. Therefore, calcination at a higher temperature of 800°C should be satisfactory in the formation of a pure perovskite phase in the samples. The results indicate the occurrence of an auto-catalytic process during the oxidative decomposition of the precursor gel. This result is in agreement with the results of Conceicao et al. [26].

3.3. Structural and Phase Analysis

Figures 2a–2c show the XRD patterns of the samples. Only $La_{0.8}Ag_{0.15}MnO_3$ sample (Fig. 2a) produced mainly single perovskite phase (with small admixture of Mn_3O_4 and La_2O_3 phases) indexed to the rhombohedral perovskite structure [*R*-3*c* (167) space group). The $La_{0.8}Ag_{0.1}MnO_3$ (Fig. 2b) and $La_{0.8}Ag_{0.2}MnO_3$ (Fig. 2c) samples had *R*-3*c* perovskite phase and much admixture of the orthorhombic structure of Ag_2O_3 (JCPDS card 77-1829), La_2O_3 and Mn_3O_4 phases. It is surprising that the $La_{0.8}Ag_{0.1}MnO_3$ sample with even lesser amounts of doped silver than the $La_{0.8}Ag_{0.15}MnO_3$ sample produced more secondary phases even though the same synthetic conditions were used. The poorly crystallized perovskite phase and presence of secondary phases in the $La_{0.8}Ag_{0.1}MnO_3$ and $La_{0.8}Ag_{0.2}MnO_3$ samples might be due to the very high exothermicity observed with glycine fuel. Kamilov et al. [27] reported that compositions like $La_{0.8}Ag_{0.15}MnO_3$ compounds with partly filled *A* sublattice in which the remaining positions are vacancies have high thermodynamic stability. Such silver-deficient compounds can be obtained with improved transport characteristics since they permit high fritting temperatures without precipitation of silver in view of their high thermodynamic stability as compared to compounds with higher silver content. Better physical properties were also recorded for $La_{0.8}Ag_{0.15}MnO_3$ manganite despite the non-stoichiometry of the composition compared to $La_{0.85}Ag_{0.15}MnO_3$ manganite [28]. In all probabilities, it is possible that the $La_{0.8}Ag_{0.15}MnO_3$ sample satisfied this requirement hence its higher crystallinity (indicating higher perovskite phase) than the other samples. The results also

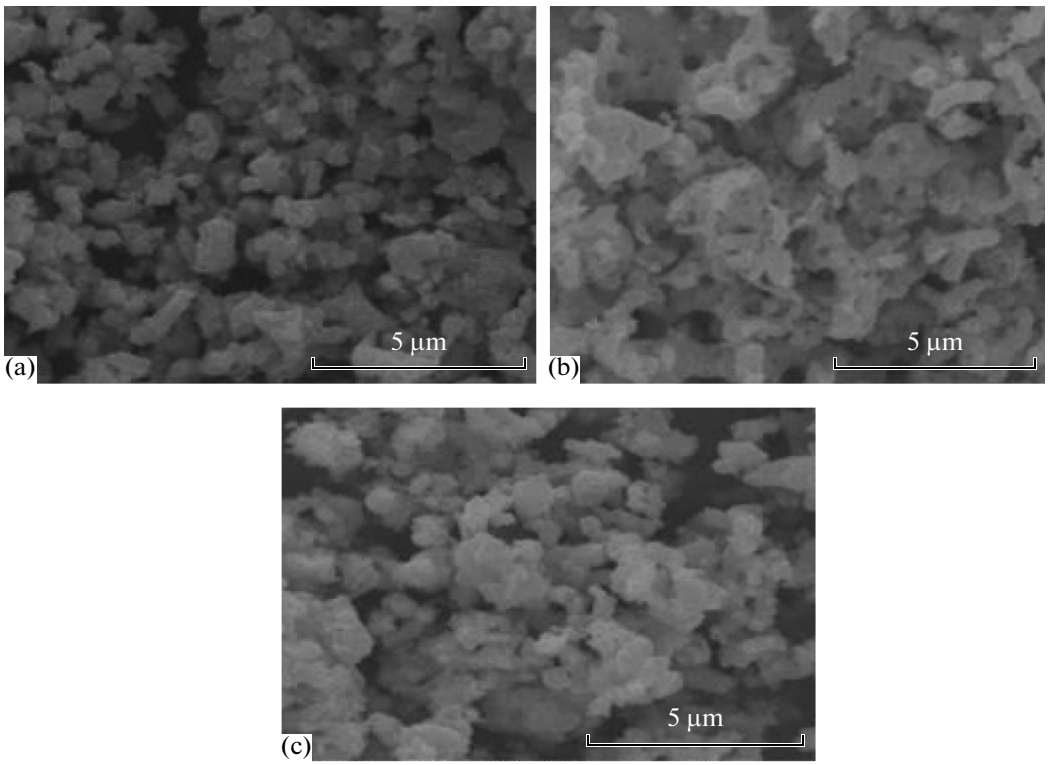

Fig. 3. SEM images of (a) $La_{0.8}Ag_{0.1}MnO_3$, (b) $La_{0.8}Ag_{0.15}MnO_3$, and (c) $La_{0.8}Ag_{0.2}MnO_3$ samples.

show that there is evidence of the insertion of silver ions in the perovskite lattice of $La_{0.85}Ag_{0.15}MnO_3$ which is lacking in the other samples. The average crystallite size obtained for $La_{0.8}Ag_{0.15}MnO_3$ sample is 48 nm. The XRD patterns of the sample show that the reflection peaks are quite broad, indicating its nano crystallinity.

3.4. Morphological and Chemical Analysis

The SEM micrographs of the samples were obtained to study their morphology and they are shown in Fig. 3. $La_{0.8}Ag_{0.15}MnO_3$ sample gave a distinct microstructure regarding porosity and density compared to the other two samples that showed similarity in shape and porosity. $La_{0.8}Ag_{0.15}MnO_3$ sample presented the most porous microstructure and was the least dense of the three samples. From the XRD analysis, $La_{0.8}Ag_{0.15}MnO_3$ sample gave the purest perovskite phase with the least impurities compared to $La_{0.8}Ag_{0.1}MnO_3$ and $La_{0.8}Na_{0.2}MnO_3$ samples and this difference seen in XRD analysis might explain the difference observed in the microstructures.

The compositional analysis of the nanocrystalline $La_{0.8}Ag_{0.15}MnO_3$ sample was carried out by EDAX and the spectrum is shown in Fig. 4. From the EDAX results the presences of La, Ag, Mn and O in the samples were confirmed. The spectrum indicates that the sample is consistent with their elemental signals and stoichiometry which are close to the nominal composition thereby having a broad homogeneity area.

3.5. Magnetic Studies

The magnetic moments as a function of applied field for the $La_{1-x}Ag_yMnO_3$ samples obtained from room temperature VSM measurements are shown in Fig. 5. The shape of the magnetization curve reveals that the $La_{0.8}Ag_{0.15}MnO_3$ sample is ferromagnetic while the $La_{0.8}Ag_{0.1}MnO_3$ and $La_{0.8}Ag_{0.2}MnO_3$ samples are paramagnetic in nature. Only the $La_{0.8}Ag_{0.15}MnO_3$ sample (Fig. 5b) produced very broad hysteresis which is consistent with the high crystallinity of the perovskite phase obtained from XRD results. This weaker magnetization seen in these samples ($La_{0.8}Ag_{0.1}MnO_3$ and $La_{0.8}Ag_{0.2}MnO_3$) might be due to the poorly crystallized magnetic perovskite phase and the admixture of secondary phases (which is over 50% in the samples) seen in their XRD compared with $La_{0.8}Ag_{0.15}MnO_3$ sample. The presence of these secondary phases also attests to the poor insertion of silver resulting in the poorly crystallized magnetic phases in $La_{0.8}Ag_{0.1}MnO_3$ and $La_{0.8}Ag_{0.2}MnO_3$ samples. The saturation magnetization, remanence, and coercivity of $La_{0.8}Ag_{0.15}MnO_3$ sample are 26 emu/g, 8 emu/g, and 150 G, respectively. The saturation magnetization

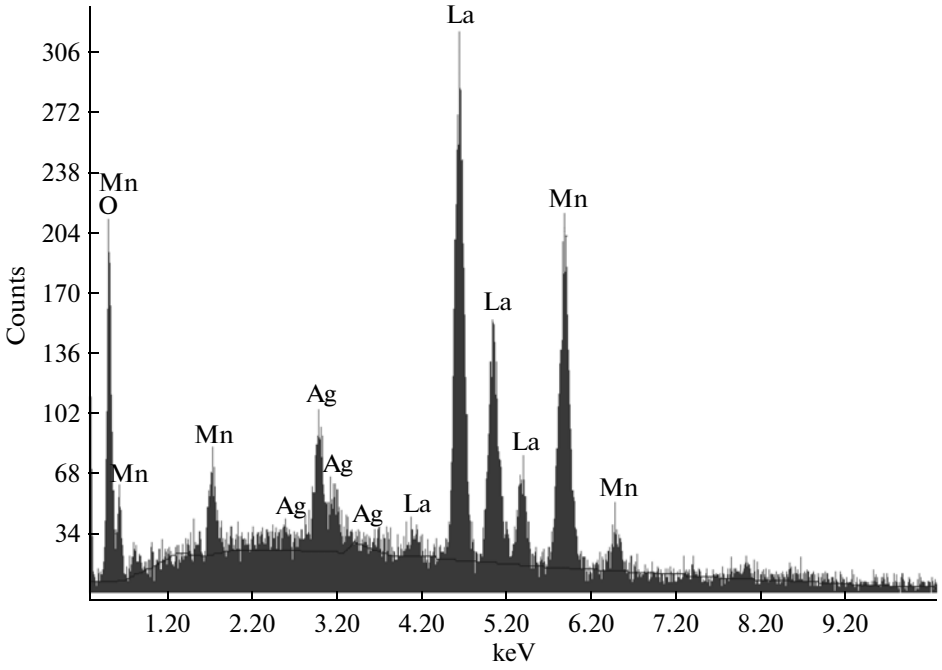

Fig. 4. EDAX spectrum of $La_{0.8}Ag_{0.15}MnO_3$ sample.

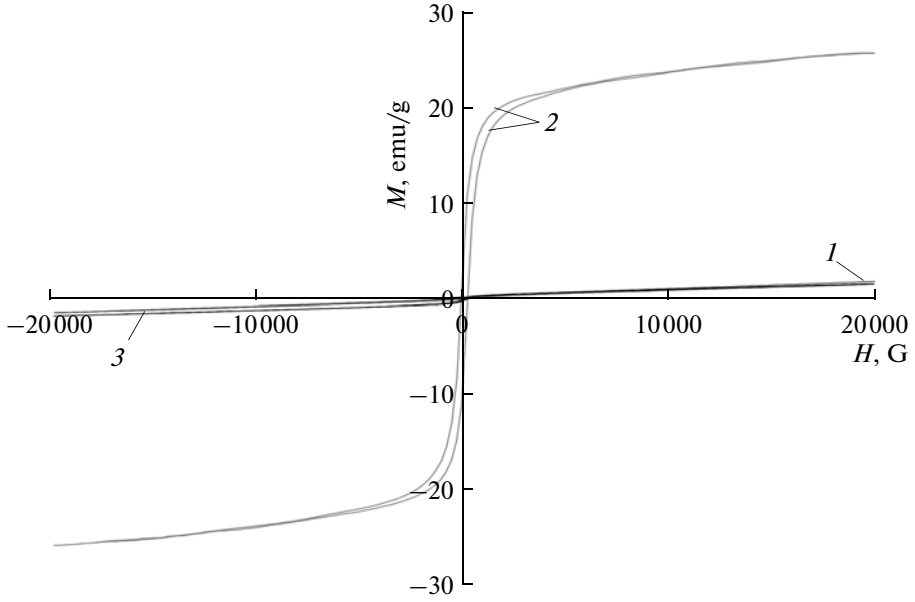

Fig. 5. VSM curves for (*1*) $La_{0.8}Ag_{0.1}MnO_3$, (*2*) $La_{0.8}Ag_{0.15}MnO_3$, and (*3*) $La_{0.8}Ag_{0.2}MnO_3$ samples.

value of the $La_{0.8}Ag_{0.15}MnO_3$ sample obtained in this study compares with the value reported for $La_{0.85}Ag_{0.15}MnO_3$ sample obtained by the oxalyl dihydrazide aided combustion synthesis [24]. The ferromagnetism seen in Ag-doped manganites comes from the doping of the parent perovskite manganite ($LaMnO_3$) by the replacement of La with Ag.

CONCLUSIONS

Low temperature auto-combustion synthesis of Ag-doped lanthanum manganite perovskite nanoparticles is reported. The use of glycine as a fuel only produced mainly single perovskite phase with the $La_{0.8}Ag_{0.15}MnO_3$ sample but had mixed phases in $La_{0.8}Ag_{0.1}MnO_3$ and $La_{0.8}Ag_{0.2}MnO_3$ samples. The nearly

monophasic perovskite structure of $La_{0.8}Ag_{0.15}MnO_3$ sample accounted for its higher magnetic properties compared with the other two samples that recorded secondary phases in the XRD and were paramagnetic in nature. From the results of this study, it will be very important to study the effect of glycine fuel composition, sintering time and temperature on the evolution of the rhombohedral perovskite phase of Ag-doped manganites hence, further investigations are required.

ACKNOWLEDGMENTS

This work would not have been possible without the visiting research grant given to Dr. C.O. Ehi-Eromosele by the International Centre for Materials Science, Jawarharlal Nehru Centre for Advanced Scientific Research, Bangalore, India. The corresponding author (C.O.E.E.) is grateful to Prof. Vikram Jayaram, Chairman of the Department of Materials Engineering, Indian Institute of Science (IISc), Bangalore for giving him access to their VSM and TG-DTA facilities.

REFERENCES

1. Coey, J.M.D., Viret, M., and von Molnar, S., Mixed-valence manganites, *Adv. Phys.*, 1999, vol. 48, no. 2, pp. 167–293; DOI: 10.1080/000187399243455.
2. Tan, G., Zhang, X., and Chen, Z., Colossal magnetoresistance effect of electron-doped manganese oxide thin film $La_{1-x}Te_xMnO_3$ ($x = 0.1, 0.15$), *J. Appl. Phys.*, 2004, vol. 95, no. 11, pp. 6322–6324; DOI: 10.1063/1.1736311.
3. So, J.H., Gladden, J.R., Hu, Y.F., Maynard, J.D., and Li, Q., Measurements of elastic constants in thin films of colossal magnetoresistance material, *Phys. Rev. Lett.*, 2003, vol. 90, no. 3, 036103; DOI: 10.1103/PhysRevLett.90.036103.
4. Malavasi, L., Mozzati, M.C., Ghigna, P., Azzoni, C.B., and Flor, G., Lattice disorder, electric properties, and magnetic behavior of $La_{1-x}Na_xMnO_{3+\delta}$ manganites, *J. Phys. Chem., Ser. B*, 2003, vol. 107, no. 11, pp. 2500–2505; DOI: 10.1021/jp027015z.
5. Cheikh-Rouhou Koubaa, W., Koubaa, M., and Cheikhrouhou, A., Effect of potassium doping on the structural, magnetic and magnetocaloric properties of $La_{0.7}Sr_{0.3-x}K_xMnO_3$ perovskite manganites, *J. Alloys Comp.*, 2009, vol. 470, nos. 1–2, pp. 42–46; DOI: 10.1016/j.jallcom.2008.03.033.
6. Tang, T., Cao, Q.Q., Gu, K.M., Xu, H.Y., Zhang, S.Y., and Du, Y.W., Giant magnetoresistance of the $La_{1-x}Ag_xMnO_3$ polycrystalline inhomogeneous granular system, *Appl. Phys. Lett.*, 2000, vol. 77, no. 5, p. 723; http://dx.doi.org/10.1063/1.127098.
7. Wang, Z.M., Tang, T., Wang, Y.P., Zhang, S.Y., and Du, Y.W., Room temperature large magnetoresistance and magnetocaloric properties of $La_{0.78}Ag_{0.22}MnO_3$ film, *J. Magn. Magn. Mater.*, 2002, vol. 246, nos. 1–2, pp. 254–258; DOI: 10.1016/S0304-8853(02)00063-X.
8. Jirak, Z., Hejtmanek, J., Knizek, K., Marysko, M., Pollert, E., Dlouha, M., Vratislav, S., Kuzel, R., and Hervieu, M., Structure and magnetism in the $Pr_{1-x}Na_xMnO_3$ perovskites ($0 \le x \le 0.2$), *J. Magn. Magn. Mater.*, 2002, vol. 250, pp. 275–287; DOI: 10.1016/S0304-8853(02)00409-2.
9. Tang, T., Gu, K.M., Cao, Q.Q., Wang, D.H., Zhang, S.Y., and Du, Y.W., Magnetocaloric properties of Ag-substituted perovskite-type manganites, *J. Magn. Magn. Mater.*, 2000, vol. 222, nos. 1–2, pp. 110–114; DOI: 10.1016/S0304-8853(00)00544-8.
10. Hien, N.T. and Thuy, N.P., Preparation and magnetocaloric effect of $La_{1-x}Ag_xMnO_3$ ($x = 0.10–0.30$) perovskite compound, *Physica, Ser. B*, 2002, vol. 319, nos. 1–4, pp. 168–173; DOI: 10.1016/S0921-4526(02)01118-3.
11. Gamzatov, A.G., Aliev, A.M., Batdalov, A.B., Abdulvagidov, Sh.B., Melnikov, O.V., and Gorbenko, O.Yu., Magnetocaloric effect in silver-doped lanthanum manganites., *Tech. Phys. Lett.*, 2006, vol. 32, no. 6, pp. 471–473; DOI: 10.1134/S1063785006060046.
12. Atsarkin, V.A., Levkin, L.V., Posvyanskiy, V.S., Melnikov, O.V., Markelova, M.N., Gorbenko, O.Y., and Kaul, A.R., Solution to the bioheat equation for hyperthermia with $La_{1-x}Ag_yMnO_{3-\delta}$ nanoparticles: The effect of temperature autostabilization, *Int. J. Hyperthermia.*, 2009, vol. 25, pp. 240–247; DOI: 10.1080/02656730802713565.
13. Melnikov, O.V., Gorbenko, O.Y., Markelova, M.N., Kaul, A.R., Atsarkin, V.A., Demidov, V.V., Soto, C., Roy, E.J., and Odintsov, B.M., Ag-doped manganite nanoparticles: new materials for temperature-controlled magnetic hyperthermia, 2009, *J. Biomed. Mater. Res., Ser. A*, vol. 91, no 4, pp. 1048–1055; DOI: 10.1002/jbm.a.32177.
14. Atsarkin, V.A., Generalov, A.A., Demidov, V.V., Mefed, A.E., Markelova, M.N., Gorbenko, O.Yu., Kaul, A.R., Roy, E.J., and Odintsov, B.M., Critical RF losses in fine particles of $La_{1-x}Ag_yMnO_{3+d}$: prospects for temperature-controlled hyperthermia, *J. Magn. Magn. Mater.*, 2009, vol. 321, no. 19, pp. 3198–3202; DOI: 10.1016/j.jmmm.2009.05.043.
15. Gorbenko, O.Yu., Markelova, M.N., Melnikov, O.V., Kaul, A.R., Atsarkin, V.A., Demidov, V.V., Mefed, A.E., Roy, E.J., and Odintsov, B.M., Synthesis, composition, and properties of the solid solutions $La_{1-x}Ag_yMnO_{3+d}$, promising materials for cell hyperthermia, *Dokl. Chem.*, 2009, vol. 424, no. 1, pp. 7–10.
16. Xu, Q.Y., Wang, R.P., and Zhang, Z., Role of Ag in $La_{1-x}Ag_xMnO_3$ manganite perovskite, *Phys. Rev., Ser. B,* 2005, vol. 71, no. 9, 092401.
17. Joly, V.L.J., Joy, P.A., and Date, S.K., Comment on "Giant magnetoresistance of the $La_{1-x}Ag_xMnO_3$ polycrystalline inhomogeneous granular system", *Appl Phys Lett.*, 2001, vol. 78, no. 23, p. 3747; http://dx.doi.org/10.1063/1.1377610.
18. Gorbenko, O.Yu., Melnikov, O.V., Kaul, A.R., Balagurov, A.M., Bushmelevab, S.N., Korolevac, L.I., and Demin, R.V., Solid solutions $La_{1-x}Ag_yMnO_{3+\delta}$: evidence for silver doping, structure and properties, *Mater. Sci. Eng., Ser. B*, 2005, vol. 116, no. 1, pp. 64–70; DOI: 10.1016/j.mseb.2004.09.013.
19. Ye, S.L., Song, W.H., Dai, J.M., Wang, K.Y., Wang, S.G., Zhang, C.L., Du, J.J., Sun, Y.P., and Fang, J., Effect of Ag substitution on the transport

1 property and magnetoresistance of $LaMnO_3$, *J. Magn. Magn. Mater.*, 2002, vol. 248, no. 1, pp. 26–33; DOI: 10.1016/S0304-8853(02)00017-3.

20. Cheikh-Rouhou Koubaaa, W., Koubaaa, M. and Cheikh-Rouhou, A., Effects of silver doping upon the physical properties of $La_{0.7}Sr_{0.3-x}Ag_xMnO_3$ manganese oxide, *J. Magn. Magn. Mater.*, 2007, vol. 316, no. 2, pp. 648–651; DOI: 10.1016/j.jmmm.2007.03.077.
21. Battabyal, M. and Dey, T.K., Low temperature electrical transport in Ag substituted $LaMnO_3$ polycrystalline pellets prepared by a pyrophoric method, *Solid State Commun.*, 2004, vol. 13, no. 5, pp. 337–342.
22. Ke, W., Zhang, N., Geng, T., and Gao, R., Discussion again of the magnetic and transport property of Ag-doped $LaMnO_3$, *J. Magn. Magn. Mater.*, 2007, vol. 312, no. 2, pp. 430–434; DOI: 10.1016/j.jmmm.2006.11.191.
23. Nikam, S.K. and Athawale, A.A., Phase formation study of noble metal (Au, Ag and Pd) doped lanthanum perovskites synthesized by hydrothermal method, *Mater. Chem. Phys.*, 2015, vol. 155, pp. 104–112; DOI: 10.1016/j.matchemphys.2015.02.006.
24. Bellakki, M.B., Shivakumara, C., Vasanthacharya, N.Y., and Prakash, A.S., Rapid synthesis of room temperature ferromagnetic Ag-doped LaMnO3 perovskite phases by the solution combustion method, *Mater. Res. Bull.*, 2010, vol. 45, no. 11, pp. 1685–1691; DOI: 10.1016/j.materresbull.2010.06.063.
25. Nagabhushana, B.M., Sreekanth, B., Chakradhar, R.P., Ramesh, K.P., Shivakumara, C., and Chandrappa, G.T., Low temperature synthesis, structural characterization, and zero-field resistivity of nanocrystalline $La_{1-x}Sr_xMnO_{3+d}$ ($0.0 \le x \le 0.3$) manganites, *Mater. Res. Bull.*, 2006, vol. 41, no. 9, pp. 1735–1746; DOI: 10.1016/j.materresbull.2006.02.014.
26. da Conceicao, L., Ribeiro, N.F.P., Furtado, J.G.M., and Souza, M.M.V.M., Effect of propellant on the combustion synthesized Sr-doped $LaMnO_3$ powders, *Ceram. Int.*, 2009, vol. 35, no. 4, pp. 1683–1687; DOI: 10.1016/j.ceramint.2008.08.016.
27. Kamilov, I.K., Gamzatov, A.G., Aliev, A.M., Batdalov, A.B., Abdulvagidov, Sh.B., Melnikov, O.V., Gorbenko, O.Yu., and Kaul, A.R., Kinetic effects in Manganites $La_{1-x}Ag_yMnO_3$ ($y \le x$), *J. Exp. Theor. Phys.*, 2007, vol. 105, no. 4, pp. 774–781.
28. Abdulvagidov, Sh.B., Gamzatov, A.G., Melnikov, O.V., and Gorbenko, O.Yu., Influence of the lanthanum deficit on electrical resistivity and heat capacity of silver-doped lanthanum manganites $La_{1-x}Ag_yMnO_3$, *J. Exp. Theor. Phys.*, 2009, vol. 109, no. 6, pp. 989–996.

SPELL: 1. Ok